Progress in Oceanography 137 (2015) 470–483

Contents lists available at ScienceDirect

Progress in Oceanography

journal homepage: www.elsevier.com/locate/pocean

Temporal variability in total, micro- and nano-phytoplankton primary production at a coastal site in the Western English Channel

Morvan K. Barnes [a,1], Gavin H. Tilstone [a,*], David J. Suggett [b], Claire E. Widdicombe [a], John Bruun [a], Victor Martinez-Vicente [a], Timothy J. Smyth [a]

[a] Plymouth Marine Laboratory, Prospect Place, West Hoe, Plymouth PL1 3DH, UK
[b] Functional Plant Biology & Climate Change Cluster, University of Technology, Sydney, PO Box 123, Broadway, NSW, Australia

ARTICLE INFO

Article history:
Available online 16 May 2015

ABSTRACT

Primary productivity and subsequent carbon cycling in the coastal zone have a significant impact on the global carbon budget. It is currently unclear how anthropogenic activity could alter these budgets but long term coastal time series of hydrological, biogeochemical and biological measurements represent a key means to better understand past drivers, and hence to predicting future seasonal and inter-annual variability in carbon fixation in coastal ecosystems. An 8-year time series of primary production from 2003 to 2010, estimated using a recently developed absorption-based algorithm, was used to determine the nature and extent of change in primary production at a coastal station (L4) in the Western English Channel (WEC). Analysis of the seasonal and inter-annual variability in production demonstrated that on average, nano- and pico-phytoplankton account for 48% of the total carbon fixation and micro-phytoplankton for 52%. A recent decline in the primary production of nano- and pico-phytoplankton from 2005 to 2010 was observed, corresponding with a decrease in winter nutrient concentrations and a decrease in the biomass of *Phaeocystis* sp. Micro-phytoplankton primary production (PP_M) remained relatively constant over the time series and was enhanced in summer during periods of high precipitation. Increases in sea surface temperature, and decreases in wind speeds and salinity were associated with later spring maxima in PP_M. Together these trends indicate that predicted increases in temperature and decrease in wind speeds in future would drive later spring production whilst predicted increases in precipitation would also continue these blooms throughout the summer at this site.

1. Introduction

Photosynthesis by phytoplankton fixes atmospheric CO_2 to form the basis of marine food webs and thus modelling and predicting this process is recognised as a central requirement for effective management of coastal resources (Tett et al., 2003). Conventional monitoring of photosynthetic biomass and production fails to sample on appropriate temporal scales to determine the impact of human activity on phytoplankton dynamics (Henson et al., 2010); as such, a step change in approach in monitoring via optical or acoustic based instrumentation, coupled to earth observation, modelling and semi-autonomous sampling, is critical to enhance the spatial and temporal frequency of observations. In coastal waters, this goal is particularly challenging as a result of optical signatures heavily influenced by non-biological particles (Sathyendranath et al., 1989; Tilstone et al., 2005), physically complex waters (e.g. Sharples et al., 2001) as well as an inherent lack of long-term observations required to distinguish natural variations from anthropogenic-driven changes in the underlying phytoplankton dynamics (Araujo et al., 2006; Le Quere et al., 2003). Temporal variability in primary production is ultimately driven by a complexity of facets operating across a range of scales, notably temperature (Harding et al., 1986), nutrients (Kyewalyanga et al., 1998), turbulence (Lewis et al., 1984) and irradiance intensity (Cote and Platt, 1984), as well as biological factors such as community structure (Cote and Platt, 1984) and physiological state (Platt and Sathyendranath, 1993), which together are strongly regulated in coastal systems by the physical structure of the water column (e.g. Sharples et al., 2001). Whilst the L4 time series in the WEC provides a means to combine long-term monitoring with shorter-scale process-studies (Southward et al., 2005) research to date has focused on characterising temporal variability of optical characteristics (Groom et al., 2009; Martinez-Vicente et al., 2010), phytoplankton (Llewellyn et al., 2005; Widdicombe et al., 2010), zooplankton (Eloire et al., 2010), and fish species

* Corresponding author.
E-mail address: ghti@pml.ac.uk (G.H. Tilstone).
[1] Current address: CNRS, Laboratoire d'Oceanographie de Villefranche, Villefranche-sur-Mer, France.

http://dx.doi.org/10.1016/j.pocean.2015.04.017
0079-6611/

composition (Genner et al., 2010) but not how these scale to variability of primary productivity. Seasonal production of phytoplankton in this area has seldom been measured with only recent observations conducted between 2009–2011 (Barnes et al., 2014) and during 2001 (Woods, 2003). Consequently, our understanding of the characteristics and drivers of inter-annual and seasonal variability in primary production in the WEC remains extremely limited with most historic observations restricted to temporally-isolated blooms (Garcia and Purdie, 1994; Holligan et al., 1984).

Phytoplankton size structure is a key trait governed by resource availability (irradiance, nutrients; e.g. Bouman et al., 2005) and grazing pressure (Peter and Sommer, 2012) to inherently determine the food-web organisation and biogeochemical functioning of pelagic ecosystems (Maranon, 2009). Measurements of size-fractionated primary production have been increasingly used to reveal the varying contributions of different size classes to total production in both coastal and open ocean systems (Huete-Ortega et al., 2011; Tilstone et al., 1999). Size-class based approaches to estimate primary production have been developed in an effort to better predict temporal and spatial variability relevant to ecosystem and biogeochemical scale processes (Hirata et al., 2009; Kameda and Ishizaka, 2005). A major advance in understanding community drivers of production is the partitioning of primary production into different size groups (Sieburth et al., 1978), which has also been aided by analysis of ocean colour models of size fractionated production (Brewin et al., 2010b) and ecosystem models (Araujo et al., 2006). Specific models of size-fractionated primary production have now been developed for both open ocean (Uitz et al., 2008) and coastal waters (Barnes et al., 2014); however, sufficient data sets still do not exist to fully understand which factors govern the seasonal and inter-annual variability in production for different size fractions (Uitz et al., 2008) and efforts to predict carbon transfer through coastal food webs thus remain exceptionally limited (Bauer et al., 2013).

We have recently demonstrated how a novel "absorption based" method can derive total as well as size fractionated (micro- and nano + pico-) phytoplankton production in coastal waters. Specifically, this method extrapolates the absorption coefficient (the peak at red wavelengths) of phytoplankton and production quantified at the sea surface to yield integrated water column fields of primary production for each size class, and is accurate to within 8% and 22% for the WEC and North Sea, respectively. This level of accuracy is unprecedented for primary production models (see Barnes et al., 2014) and thus our approach provides a unique means to examine how the environment regulates temporal variation in primary production where bio-optical data is readily available. Here, we apply the Barnes et al. (2014) absorption-based model of coastal primary production to an 8-year time series of weekly *in situ* phytoplankton absorption measurements to specifically determine what (and how) environmental factors control the seasonal and inter-annual variability in surface, depth-integrated and size-fractionated primary production.

2. Materials and methods

2.1. Study site and sampling

Samples were collected from station L4 (50°15′N, 4°13′W; Fig. 1) weekly from January 2003 to December 2010 aboard RV Quest. On reaching the station, a Lagrangian mode was used whereby the ship was allowed to drift with the water body being sampled. The tide at the site has a maximum range of 5.4 m and a current of 0.55 m s^{-1} (Pingree, 1980). The river Tamar is the main source of freshwater flowing into the WEC with a range of 5–140 m^3 s^{-1} at its mouth (Uncles and Stephens, 1990). The sampling regime included different phases of the tidal cycle depending on the time the ship reached the station. Vertical profiles of temperature and fluorescence were obtained from SeaBird SBE19 + CTD casts. Mixed layer depth (MLD) was estimated from the density profiles following Levitus (1982). Water samples were collected from 10L Niskin bottles for the measurement of phytoplankton absorption, pigments and abundance, and primary production. For phytoplankton pigments, 1 L aliquots of seawater were filtered onto 0.47 μm glass-fibre filters for pigment analysis by reversed-phase high-performance liquid chromatography. Samples for phytoplankton species composition and carbon concentrations were collected from a depth of 10 m and analysed by light microscopy following Widdicombe et al. (2010). Cell volumes were calculated using approximate geometric shapes (Widdicombe et al., 2002) and converted to biomass using the equations of Menden-Deuer and Lessard (2000).

2.2. Absorption and production

The light absorption coefficient for phytoplankton at 665 nm (a_{ph}, m^{-1}) was determined using the filter-pad transmission-reflectance technique (Tassan and Ferrari, 1995, 1998). 1 L aliquots of seawater from surface, 10, 25 and 50 m were filtered onto 0.47 μm glass-fibre filters. Chlorophyll-a (Chl *a*) specific absorption coefficients ($a^*_{ph}(\lambda)$) were calculated by dividing $a_{ph}(\lambda)$ by the respective HPLC Chl *a* concentration. Photosynthetically active radiation (E_{PAR}) was calculated using the approach of Gregg and Carder (1990) modified to include the effects of clouds (Reed, 1977) and using wind speed and percentage cloud cover from the European Centre for Medium Range Weather Forecasting (ECMWF) ERA-40 dataset for the grid point closest to the location of L4, as in Smyth et al. (2010).

Surface primary production PP_0 (mg C m^{-3} d^{-1}) and depth-integrated production PP_{eu} (mg C m^{-2} d^{-1}) were measured from 2009–2010 using Photosynthesis-Irradiance curves in linear photosynthetrons following Tilstone et al. (2003). Surface (PP_0) and euphotic depth-integrated production PP_{eu} were also estimated for 2003–2010 from $a_{ph}(665)$ and E_{PAR} using the equations given in Barnes et al. (2014) as follows:

$$PP_0 = 145.3 \times (E_{PAR} \times a_{ph}\{665\}) - 2.6 \quad (1)$$

$$\text{Log } PP_{eu} = 0.915 \times \int (0 - 50m)\text{Log}(E_{PAR} \times a_{ph}\{665\}) + 2.08 \quad (2)$$

Compared to an independent data set of *in situ* PP_{eu}, the model has a high prediction capability, evident by a small RMSE (0.021 Log_{10}(mol C m^{-2} d^{-1})) and low scatter from least squares linear regression ($R^2 = 0.71$), a slope close to 1 (see Fig. 9a in Barnes et al., 2014) and low relative and absolute percentage difference indicating minimum bias and uncertainty.

Surface production (mg C m^{-3} d^{-1}) for micro-phytoplankton (PP_M) and for combined nano- and pico-phytoplankton (PP_{NP}) were also estimated from $a_{ph}(665)$ and E_{PAR} also following the approach of Barnes et al. (2014):

$$PP_0\{M\} = 171.5 \times (E_{PAR} \times a_{ph}\{665, M\}) - 5.53 \quad (3)$$

$$PP_0\{NP\} = 163.5 \times \text{Log}(E_{PAR} \times a_{ph}\{665, NP\}) + 10.4 \quad (4)$$

where *M* indicates micro- and NP is nano- + pico-. There was no significant difference in the relationship between Chl *a* and

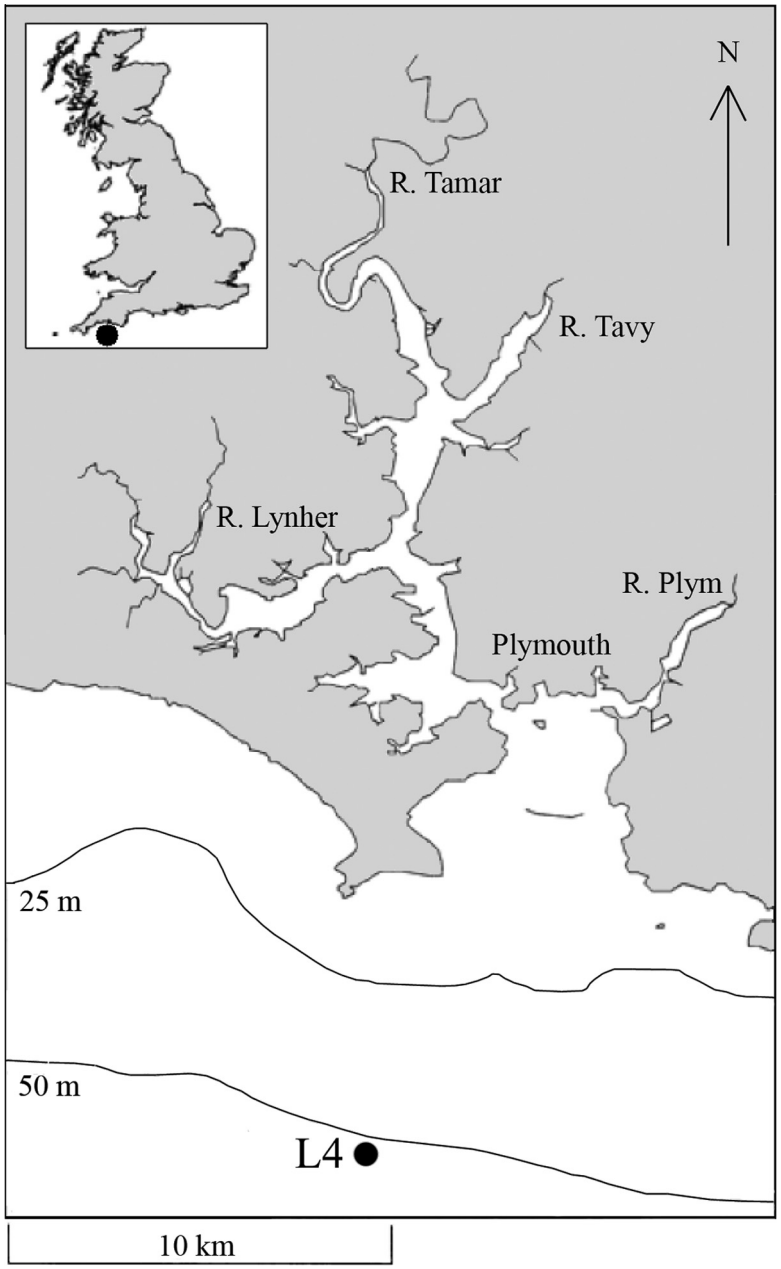

Fig. 1. Station L4 situated in the Western English Channel off the coast of Plymouth and the Tamar estuary.

$a_{ph}(665)$ for total Chl *a*, micro- and nano + pico phytoplankton when these size fractions were >50% of the Chl *a* biomass, indicating that absorption in these size fractions at 665 nm is linearly related to Chl *a*. The relationship between depth-specific production PP_z and phytoplankton light absorption ($E_{PAR} \times a_{ph}(665)$) for both PP_M and PP_{NP} is given in Barnes et al. (2014). For both size fractions a strong linear regression was observed which explained 82% and 87% of PP_M and PP_{NP}, respectively (see Table 1; Eqs. 13–14 in Barnes et al., 2014). The size limit of PP_M is >10 μm and of PP_{NP} is 0.2–10 μm.

Total annual and spring annual production were calculated from PP_{eu} data as the integral of linearly-interpolated data for the whole year and for the spring period from 21st March to 21st June of each year. Winter and summer seasons were defined from solstice to equinox; spring and autumn were defined from equinox to solstice.

Table 1
Annual totals of PP_{eu} (g C m^{-2}) and PP_0, PP_M and PP_{NP} (g C m^{-3}).

	2003	2004	2005	2006	2007	2008	2009	2010	Mean
ΣPP_{eu}	113	105	121	124	99	91	128	118	112
ΣPP_0	15.2	14.8	18.0	17.1	14.6	15.0	16.0	9.9	15.1
ΣPP_M	6.6	6.8	9.5	9.4	8.4	8.5	9.1	5.2	7.9
ΣPP_{NP}	8.6	8.0	8.5	7.7	6.2	6.6	6.9	4.7	7.1

2.3. Statistical analysis

Dependence of primary productivity upon biological and environmental variables was examined using principal components analysis (PCA) to enable visualisation of the similarities and differences between samples, as well as the correlations between the environmental, biological and photo-physiological variables of interest. The data matrix was composed of 212 individual

temporally-separated samples and 15 variables. These were PP_M, PP_{NP}, sea surface temperature (SST), salinity, MLD, nitrate, phosphate and silicate concentrations, and the carbon biomass of diatoms, dinoflagellates, coccolithophores and flagellates. Prior to analysis, data were mean-centred and normalised to one standard deviation to allow for comparison of variables with different units and dispersions.

Stepwise multiple linear regressions were used to identify predictors of PP_0, PP_{eu}, PP_M and PP_{NP} from a database of environmental data that included those parameters listed above but also daily PAR, wind speed, wind direction and rainfall. All data were checked for normal distributions using Kolomogrov–Smirnov test and transformed to normality by log or square root. Kruskal–Wallis one-way analysis of variance tests were performed on a_{ph} to determine the inter-annual variability.

The a_{ph}, PP_M and PP_{NP} time series were analysed using an Auto-Regressive Integrated Moving Average (ARIMA) transfer function model (Bruun et al., 2012; Shumway and Stoffer, 2010). This method allows the frequency spectrum of the time series to be examined to identify the dominant repeat cycles in the time series. Longer-term trend components, if present, appear in the spectrum as a very low frequency term, which indicates a slow steady change. The magnitude and significance of these terms, including the presence of a linear trend which was estimated with the transfer function model using maximum likelihood optimisation (Bruun et al., 2012). To further analyse significant trends in the time series, an analysis of the seasonal anomalies was performed, where the anomaly was calculated from the difference between the climatological (2003–2010) and yearly means.

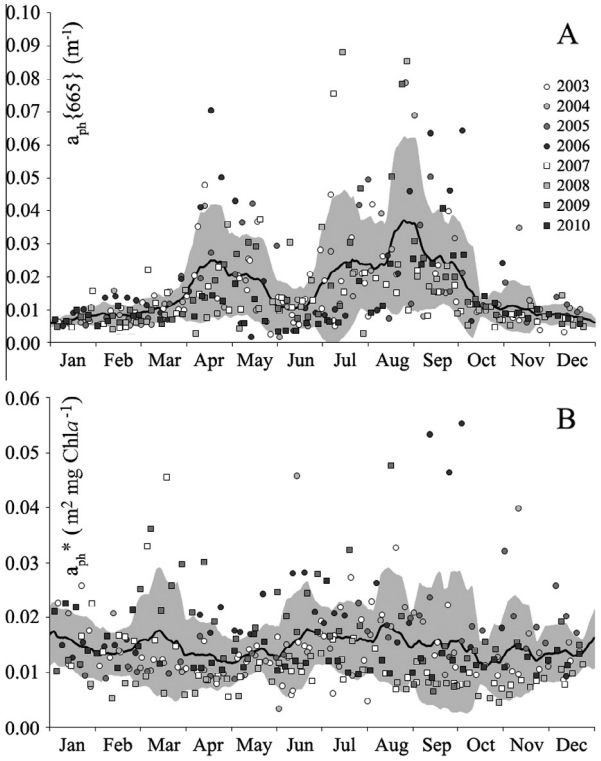

Fig. 2. Climatology of (A) $a_{ph}(665)$ and (B) $a^*_{ph}(665)$ from 2003–2010. 10-day running mean is shown as the black line; the grey area represents the standard deviation above and below the mean. Data for individual years are also overlaid details of which are given in the legend.

3. Results

3.1. Seasonality of phytoplankton absorption

At L4 from 2003–2010, $a_{ph}(665)$ averaged ca. 0.01 m^{-1} during the late autumn and winter and also during June (Fig. 2A). During the spring bloom, from April to May mean $a_{ph}(665)$ increased to 0.021 (±0.014) m^{-1} with a peak absorption of 0.071 m^{-1} in 2006; however, the highest observations of $a_{ph}(665)$ occurred during summer. From July to September, mean $a_{ph}(665)$ was 0.026 (±0.019) m^{-1} with the 10-day mean reaching 0.037 m^{-1} during late August. During this period several observations over 0.060 m^{-1} were recorded in 2004, 2006, 2007, 2009 with a peak absorption of 0.88 m^{-1} in 2008. Two-thirds of summer observations of $a_{ph}(665)$ were below 0.026 m^{-1} and the highest variability in phytoplankton absorption occurred during this period.

In contrast to $a_{ph}(665)$, phytoplankton absorption normalised to chlorophyll *a* (a^*_{ph}) showed a much less obvious seasonal component (Fig. 2B). Across the 8-year time series, mean a^*_{ph} was 0.015 (±0.007) m^2(mg Chl *a*)$^{-1}$ with over 80% of observations <0.019 m^2 mg Chl *a*. Maximum a^*_{ph} was observed in September 2006, when a^*_{ph} reached 0.055 m^2(mg Chl *a*)$^{-1}$. The 10-day running mean showed little variation reaching a maximum of 0.019 m^2(mg Chl *a*)$^{-1}$ in August and a minimum of 0.011 m^2(mg Chl *a*)$^{-1}$ in October. Such variability possibly reflects the effect of pigment packaging, which for samples with high biomass would result in a decoupling between the concentration of light absorbing pigments (such as Chl *a*) and the extent with which these pigments can absorb light.

No significant inter-annual differences in $a_{ph}(665)$ were found for summer ($H = 5.58$, $p = 0.589$), autumn ($H = 9.98$, $p = 0.190$) or winter ($H = 9.28$, $p = 0.233$). However, spring $a_{ph}(665)$ varied significantly between years ($H = 14.56$, $p = 0.042$) with higher absorption particularly for 2005 and 2006 (Fig. 3). Although there was a large variation in the timing of the summer $a_{ph}(665)$ maximum between years (Fig. 3), its magnitude remained comparatively constant.

3.2. Time series of primary production

Surface water primary production, calculated from $a_{ph}(665)$ are shown for 2003–2010 (Fig. 4). There was a very tight match between modelled and *in situ* PP_0. Throughout this period, mean PP_0 was 43.3 mg C m^{-3} d^{-1} but varied between 3.0 and 279 mg C m^{-3} d^{-1}. In winter and the latter half of autumn, PP_0 was typically <35 mg C m^{-3} d^{-1} with a mean PP_0 of just 12.7 (±7.1) mg C m^{-3} d^{-1}. However, during spring mean PP_0 increased to 56 (±43) mg C m^{-3} d^{-1} with an average annual maximum spring production of 140 (±43) mg C m^{-3} d^{-1}. The initial spring time PP_0 maximum occurred between 14th April (in 2003) and 21st May (in 2007). This PP_0 maximum generally corresponded with a bloom of one species of diatom (e.g. *Guinardia* sp., *Chaetocerosdebilis*) or flagellate (e.g. *Phaeocystis* sp.) although with varying degrees of dominance. The highest PP_0 in spring was observed in April 2006 equivalent to a carbon fixation of 188 mg C m^{-3} d^{-1} during a mono-specific bloom of *Guinardia* sp., whilst maximum surface production in spring 2010 was only 58 mg C m^{-3} d^{-1}.

Surface production was even higher in summer compared with spring with a mean PP_0 of 74 (±53) mg C m^{-3} d^{-1} and a mean summer maximum of 184 (±62) mg C m^{-3} d^{-1}. The timing of the summer maximum varied considerably between 9th July (in 2007) and 12th September (in 2006) as did the dominant species of the major blooms. In half of the observed years, the dinoflagellate *Karenia mikimotoi* contributed most to the carbon biomass amongst the phytoplankton community (up to 97% of the total carbon) during at least one summer peak in PP_0. Other species also contributed to one or more summer peaks during the time series including

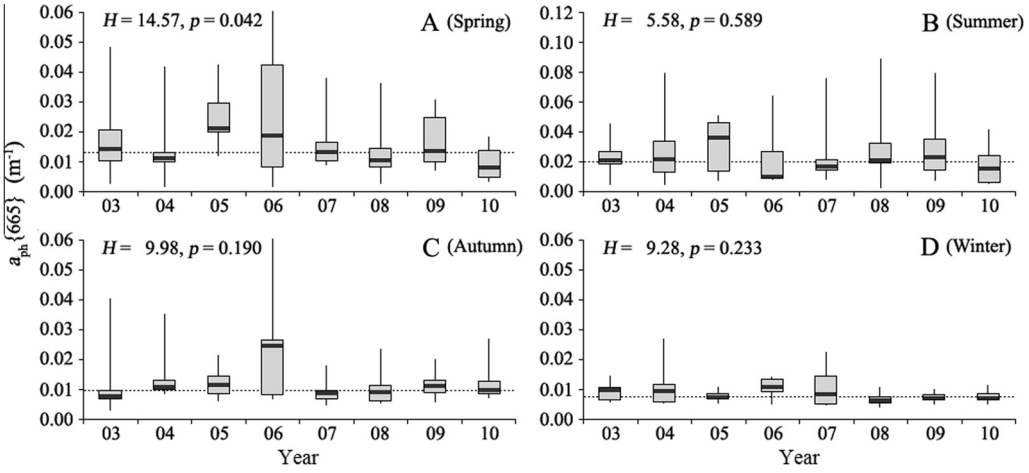

Fig. 3. Box plots showing inter-annual variability in a_{ph} from 2003–2010 for spring (A), summer (B), autumn (C) and winter (D). Means for each season are shown as dotted line. For each box the median (thick line), first and third quartiles (lower and upper box boundaries) and the minimum and maximum observations (lower and upper vertical lines) are given. Kruskal–Wallis test statistics for inter-annual variability in a_{ph} are shown for each season.

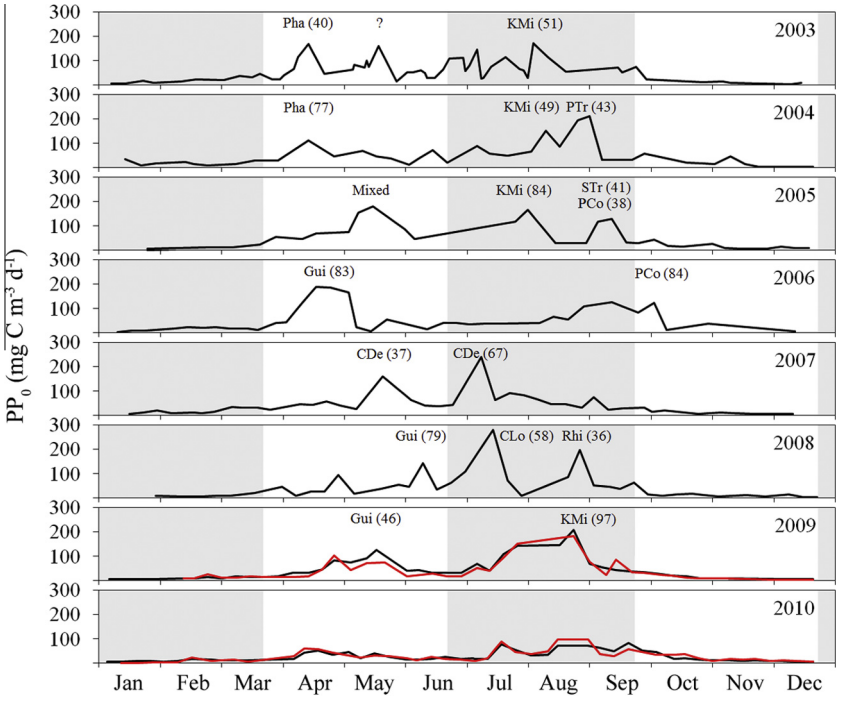

Fig. 4. Temporal changes in modelled PP_0 (mg C m^{-3} d^{-1}) at L4 from 2003–2010. *In situ* PP_0 is shown for 2009 and 2010 (red line). Phytoplankton taxa which contribute to >25% of the total phytoplankton carbon (and their peak percentage contribution) are shown each year for up to three peaks in PP_0 over 100 mg C m^{-3} d^{-1}. Taxa shown are diatoms *Chaetoceros debilis* (CDe), *Guinardia* sp. (Gui), *Rhizosolenia setigera* (Rhi), dinoflagellates *Ceratium longipes* (CLo), *Karenia mikimotoi* (KMi), *Prorocentrum cordatum* (PCo), *Prorocentrum triestinum* (PTr), *Scripsiella trochoidea* (STr) and flagellate *Phaeocystis* sp. (Pha). Shading delimits different seasons. (For interpretation of the references to colour in this figure legend, the reader is referred to the web version of this article.)

diatoms *Chaetoceros debilis* and *Rhizosolenia* sp. and dinoflagellates *Ceratium longipes*, *Prorocentrum cordatum*, *Prorocentrum triestinum* and *Scripsiella trochoidea*. The highest summertime PP_0 was 279 mg C m^{-3} d^{-1} in a July 2008 bloom of *Ceratium longipes*. Lower summer peaks of between 75 and 53 mg C m^{-3} d^{-1}were observed in 2006 and 2010, respectively, although a *Prorocentrum cordatum* bloom occurred in early October 2006 contributing to autumn productivity.

Depth-integrated primary production PP_{eu} showed similar seasonal profiles to PP_0 with similar peaks and contributing taxa (data not shown). Mean PP_{eu} was higher in summer (591 ± 296 mg C m^{-2} d^{-1}) than in spring (363 ± 195 mg C m^{-2} d^{-1}) and PP_{eu} was much lower in autumn and winter (data not shown). Seasonal anomalies of PP_{eu} were less than ±94 mg C m^{-2} d^{-1} and less than ± 38% with the exception of autumn 2006 when mean PP_{eu} was 261 mg C m^{-2} d^{-1} (159%) above the 8-year autumn mean. There was also a good match between modelled and *in situ* PP_0, PP_M and PP_{NP} (Fig. 5). PP_M and PP_{NP} were characterised by very different seasonal and inter-annual trends. PP_M and PP_{NP} exhibited comparable means over the 8-year time series (15.5 ± 18.8 and 14.2 ± 13.3 mg C m^{-3} d^{-1} respectively; Fig. 5) suggesting that micro-phytoplankton and lower size classes contribute almost equally to PP_0.

The harmonic terms of the $a_{ph}(665)$ time series explained 31% of the variability in $a_{ph}(665)$, with significant 12, 6 and 4 monthly terms in the fitted model (Fig. 6B). The sub-annual harmonics were

quite distinct, indicating the presence of repeating sub-annual characteristics, explained by the bi-modal peak in the climatology of $a_{ph}(665)$ in Fig. 2A. For PP_{NP}, the harmonic terms explained 44% of the variability in the time series with significant 12, 6 and 4 monthly terms in the fitted model (Fig. 6D). There was a significant underlying and negative linear, $\log_{10}$ scale, trend with a value of $10^{-0.12}$ (Fig. 6C). The linear trend and the annual harmonic pattern constitute the majority of the fitted model. For PP_M, the harmonic terms explained 43% of the variability from 2003–2010, with significant 12, 6 and 4 monthly terms in the fitted model. The annual and 4 month harmonic patterns constitute the majority of the fitted model (Fig. 6E), again indicating bi-modal peaks in PP_M (spring – diatoms; summer – dinoflagellates).

On a seasonal basis, mean PP_M was higher than PP_{NP} during spring and summer, whilst PP_{NP} was higher in autumn (Fig. 5). No difference was found between PP_M and PP_{NP} in winter, since PP was always low. Mean seasonal anomalies for PP_M and PP_{NP} were ±31% and ±21% respectively, suggesting higher inter-annual variability in PP_M than in PP_{NP}. The highest spring PP_M occurred in 2005 (89.3 mg C m^{-3} d^{-1}) and 2006 (82.6 mg C m^{-3} d^{-1}) and the highest mean summer PP_M was in 2008 (41.6 mg C m^{-3} d^{-1}). No clear trend was evident for PP_M from 2003–2010. Mean PP_{NP} was particularly high during summer from 2003–2005 with a maximum of 32 mg C m^{-3} d^{-1} in 2006. In both spring and summer of 2010, PP_{NP} was low 2010 (8.7 and 16.1 mg C m^{-3} d^{-1} respectively). There was a significant negative trend in the seasonal anomaly in PP_{NP} from 2003–2010 ($F_{1,32} = 14.86$, $R^2 = 0.33$, $p = 0.001$) indicating a significant decline in PP_{NP} from 2005 to 2010 (Fig. 7C).

Overall, total annual PP_{eu} (ΣPP_{eu}) at L4 varied between 91 and 128 g C m^{-2} $y^{-1}$with a low coefficient of variance of 12% (Table 1). ΣPP_0 varied almost twofold between 9.9 and 18.0 g C m^{-3} with a higher coefficient of variance than ΣPP_{eu} (16%). Although instantaneous PP_0 and PP_{eu} were strongly correlated, a low ΣPP_0 did not always result in a low ΣPP_{eu} (e.g. 2010) probably reflecting subsurface blooms. Mean ΣPP_M and ΣPP_{NP} were 7.9 (±1.5) and 7.1 (±1.3) g C m^{-3}, respectively.

3.3. Environmental and biological forcing factors on primary production

The dependence of PP_0 and the relative contributions of PP_M and PP_{NP} to PP_0 (f_M and f_{NP}, respectively) upon biological and environmental variables via the PCA eigenvalues demonstrated that the first two principal components account for <50% of the variability in the dataset (Fig. 8A). PC1 explained 34% of the variability in the dataset and PC2 explained 14%. PC1 explained the seasonal difference between samples with positive eigenvalues attributed to spring and summer samples and negative values attributed to autumn and winter samples (Fig. 8B). The main variables contributing to PC1 positive eigenvalues values were PP_0 ($R^2 = 0.58$), f_M and diatom biomass ($R^2 = 0.54$) and to a lesser extent the biomass of dinoflagellates, coccolithophores and flagellates as well as temperature (Fig. 8C). This is consistent with the seasonality of stratification and primary production in the WEC, which on the one hand is potentially governed by temperature control on enzymatic processes associated with carbon fixation (Eppley, 1972) and on the other by phytoplankton succession (Moore et al., 2005). PC1 negative values were attributed to nitrate ($R^2 = 0.58$), phosphate, silicate and f_{NP}. Thus from PC1, PP_0 and f_M, in the form of diatoms and dinoflagellates, were negatively correlated with nitrate and phosphate reflecting nutrient reduction or limitation during high biomass and primary production associated with micro-phytoplankton dominance. The main variables contributing to PC2 were f_{NP} ($R^2 = 0.49$), temperature ($R^2 = 0.18$), dinoflagellate biomass ($R^2 = 0.17$) and a^*_{ph} ($R^2 = 0.15$) with positive eigenvalues and also f_M, diatoms and MLD but with negative values. PC2 describes the temporal separation between deeper mixed layer and diatoms and a warming of the water column and high a^*_{ph} associated with dinoflagellates (Fig. 8B and C).

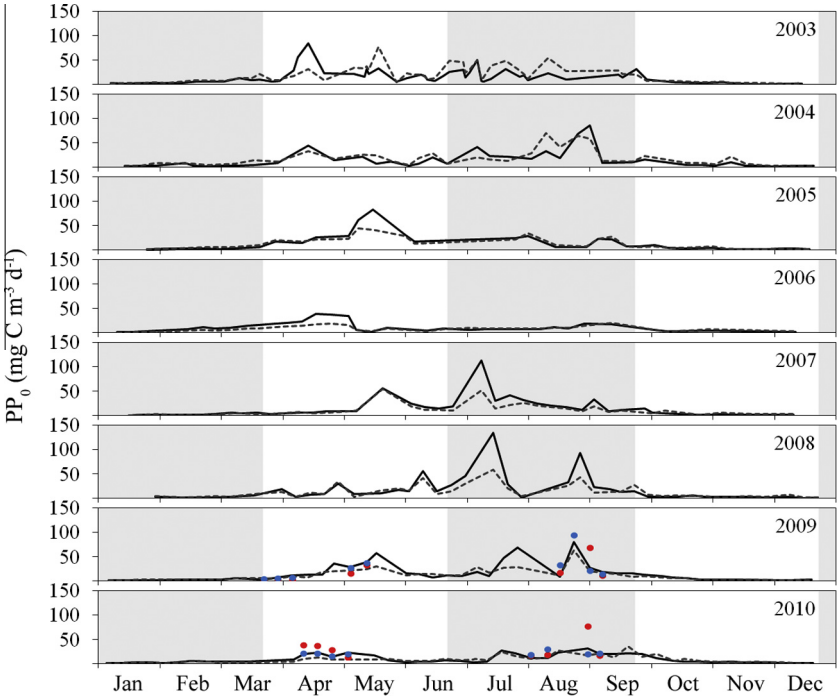

Fig. 5. Temporal variation in modelled PP_0 (mg C m^{-3} d^{-1}) in micro- (solid line) and nano- + pico-phytoplankton (dotted line) at L4 from 2003–2010. *In situ* PP_0 is also given for 2009 and 2010; red circles are micro-PP_0, blue circles are nano + pico-PP_0. (For interpretation of the references to colour in this figure legend, the reader is referred to the web version of this article.)

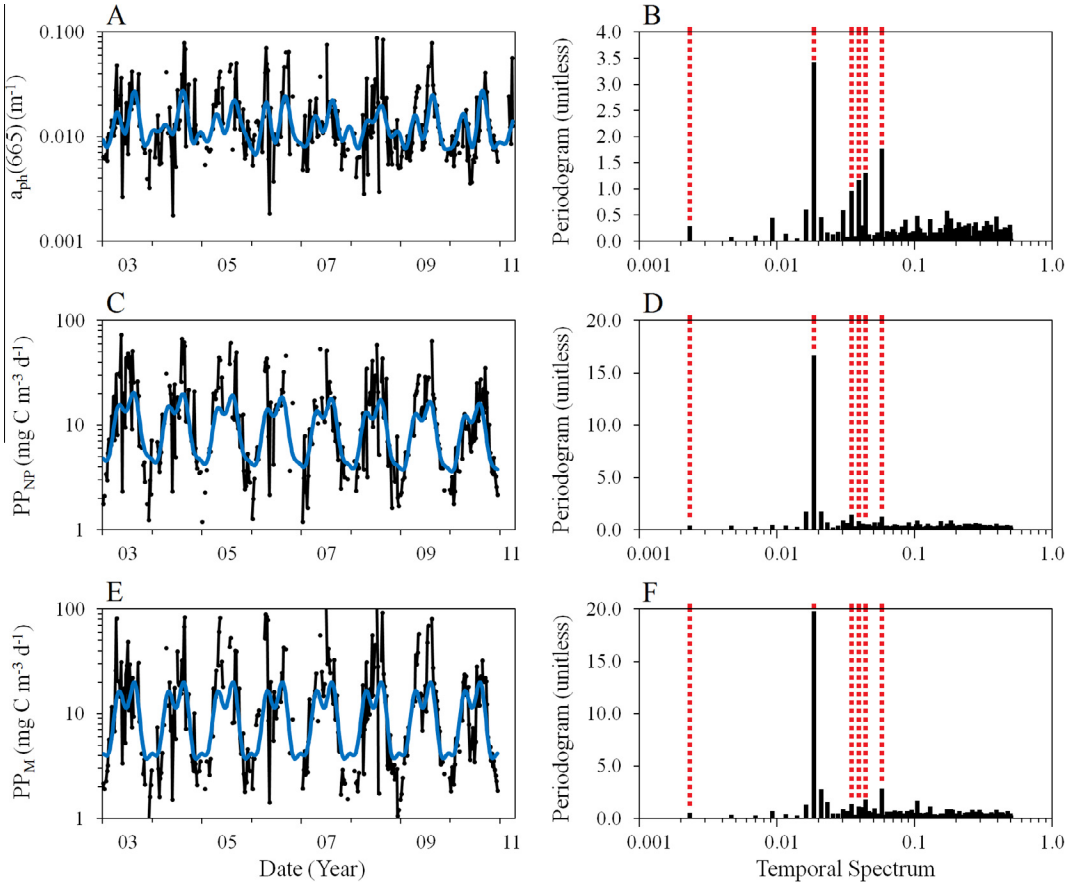

Fig. 6. Trend analysis of (A) $a_{ph}(665)$, (C) nano- & pico-primary production (PP_{NP}) and (D) micro-phytoplankton primary production (PP_M); black line is the data series, blue line is the model fit. Harmonic periodograms of (B) $a_{ph}(665)$, (D) nano- & pico-primary production and (F) micro-phytoplankton primary production from time series data. Vertical red dashed lines indicate significant harmonics. (For interpretation of the references to colour in this figure legend, the reader is referred to the web version of this article.)

Surprisingly, forward stepwise multiple regression further demonstrated that changes in diatom biomass explained a significant proportion of PP_0, PP_{eu} and PP_M variance during summer, whereas flagellate biomass was related to PP_0 and PP_{eu} during spring (Table 2). In addition, flagellate biomass was a significant predictor of production for both size groups during spring, whilst the relationship between diatom biomass and PP_M was only significant in spring and summer (Table 2). According to PC2, f_{NP} was primarily associated with dinoflagellates, coccolithophores, flagellates, temperature and a^*_{ph} suggesting that these phytoplankton classes modulate production at L4 via higher light absorption efficiency (Fig. 9). The forward stepwise regression also demonstrated that in summer, production was controlled by a^*_{ph} particularly for PP_{NP} with higher production by the smaller size classes associated with higher a^*_{ph}, thus also suggesting a higher light absorption efficiency for f_{NP}.

In summary, community structure explained the highest percentage variance in PP_0 and PP_{eu} at L4, with *Phaeocystis* sp. in spring and dinoflagellates, coccolithophores and flagellates in summer. The taxa that describe most of the variability in PP_M and PP_{NP} are shown in Table 3. Temporal variability of the diatom *Rhizosolenia* sp. explained 28.7% of the variation in PP_M throughout the time series, whilst the diatom *Guinardia delicatula* and dinoflagellate *Dinophysis* sp. explained a further 12.7% and 6.6% respectively. A total of 87% of PP_M could be explained by 38 taxa. The dinoflagellate *Karenia mikimotoi* accounted for 29.3% of the variability in PP_{NP}. *Rhizosolenia* sp. also explained a further 6.8% in the variability in PP_{NP} and a maximum of 74% could be explained by 23 taxa.

The only environmental variables that explained a significant variance in PP_0, PP_{eu} and PP_M were nitrate in spring and salinity in summer, which were negatively correlated (Table 2). This suggests that high PP at L4 (and especially in micro-phytoplankton) is strongly associated with nutrient uptake and fresh water input. Silicate was also positively correlated with PP_{NP} in summer (Table 2). Run-off from the River Tamar can result in increased concentrations of nitrate, phosphate and silicate at station L4 (Rees et al., 2009). Since nitrate and phosphate are used by nano + pico-phytoplankton, high silicate concentrations remain in the water column as a tracer of river run-off.

3.4. Forcing factors on seasonal carbon fixation budgets and phenology

To further understand the inter-annual variability in seasonal carbon budgets for both size fractions, seasonal averages of environmental and community variables were further examined using regression analyses against total spring and summer PP_M and PP_{NP} as well as the timing of the spring maximum of PP_M and PP_{NP} (Fig. 9). No average seasonal biomass of any of the phytoplankton classes tested was significantly correlated with either PP_M or PP_{NP} during spring or summer (data not shown). Average spring PP_M from 2003–2010 was significantly and negatively correlated with mean spring irradiance ($r = -0.872$, $p = 0.005$) and positively correlated with mean spring rainfall ($r = 0.754$, $p = 0.031$; Fig. 9), illustrating a

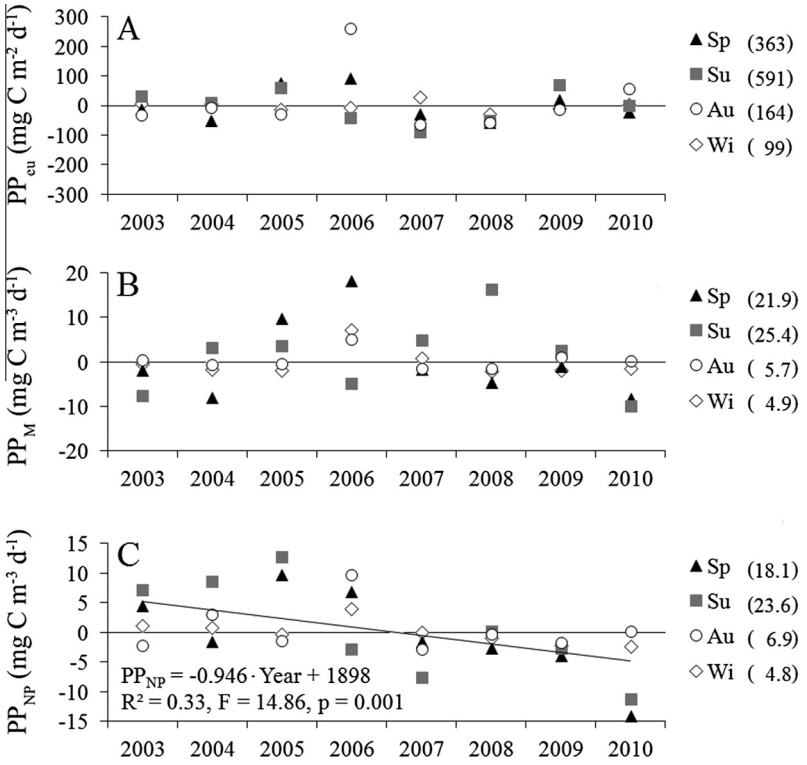

Fig. 7. Yearly seasonal anomalies in (A) PP_{eu} (mg C m^{-2} d^{-1}), (B) PP_M (mg C m^{-3} d^{-1}) and (C) PP_{NP} (mg C m^{-3} d^{-1}) from 2003–2010. For each production measurement, the seasonal mean is indicated in parentheses and must be added to the anomaly to get the total production value. A significant negative relationship between the seasonal anomalies and year was found for PP_{NP}, the statistics of which are shown (C). Sp is spring, Su is summer, Au is autumn and Wi is winter.

linkage between rainfall and cloud cover which reduces irradiance. In contrast, mean spring PP_{NP} was significantly correlated with mean winter silicate ($r = 0.725$, $p = 0.042$) but not nitrate ($r = 0.650$, $p = 0.081$). There were no significant relationships between mean summer PP_M or PP_{NP} and environmental variables. The timing of the spring PP_M maximum (PP_M^{max}), which corresponded to the first major increase in productivity in all years except for 2008) was positively correlated with salinity ($r = 0.730$, $p = 0.040$) and negatively correlated with mean wind speed ($r = -0.862$, $p = 0.006$). Thus, in years when wind speed was particularly low and with reduced salinity intrusions from the River Tamar, blooms occurred much later in the year. In years with low mean spring SST (e.g. 2006, 2010), the spring bloom occurred earlier although the relationship between PP_M^{max} and SST could not be satisfactorily explained by a significant linear regression ($r = 0.669$, $p = 0.069$). During warmer years when the wind speed was low (e.g. 2004 & 2008), which results in stronger stratification, the spring bloom production occurred later (Fig. 9E and G), presumably due to a reduction in the availability of winter nutrients under higher stratification. No significant relationships were found to explain the timing of PP_{NP}^{max}. In summary, on a weekly basis changes phytoplankton community composition had a significant effect on the temporal changes in PP (Fig 8, Table 3). On a seasonal basis, PP_M was significantly and negatively correlated with mean spring irradiance and positively correlated with mean spring rainfall, whereas PP_{NP} was significantly correlated with mean winter silicate.

4. Discussion

4.1. Seasonal and inter-annual variability in primary production in the Western English Channel

Our unique primary production time series acquired from 8 years of phytoplankton absorption observations has enabled a description of size-class specific phytoplankton production in the WEC for the first time; importantly we show for this site that annual productivity has been driven by two or more blooms within each year, and with one phytoplankton species usually dominating the carbon biomass (Fig. 4). Our finding contrasts against the "classical" view for the WEC of a single annual bloom that reaches a maximum in spring (Boalch et al., 1978) as the major driver of the annual carbon budget (Joint and Groom, 2000). Instead our data is more consistent with reports of bi-modal peaks for some regions of the NE Atlantic (McQuatters-Gollop et al., 2011; Tilstone et al., 2014); however, for L4 the secondary summer peak is often higher than the spring peak as a result of periodic dinoflagellate blooms in the summer (Barnes et al., 2015) and an overall temporal trend of declining diatom biomass in spring (Widdicombe et al., 2010). A key question at this stage is whether primary production during spring versus summer has similarly changed (Henson et al., 2010)?

Station E1 (50°02′N 4°22′W) in the WEC is further offshore than L4 but previously the focus of a long-term study of primary production from 1964–1986 (Boalch, 1987; Boalch et al., 1978). Throughout this time frame (1964–1986) mean production in April and May (ca. 1000 mg C m^{-2} d^{-1}) was >50% higher than that observed from July–September Boalch (1987). At other stations further offshore into the Channel, the relative importance of summer productivity increases and (Boalch et al., 1978) suggest it may even outweigh carbon fixation during spring in the centre of the WEC. Short-duration cruises have also observed high productivity in the centre of the Channel during summer particularly during blooms of *Karenia mikimotoi* (Garcia and Purdie, 1994; Holligan et al., 1984). Whilst the 1964–1986 E1 time series provides an indication of mean seasonality from over 23 years of observations, the temporal resolution is insufficient (between 4–10 measurements per year) to accurately yield coherent information on seasonal or inter-annual variability in carbon budgets.

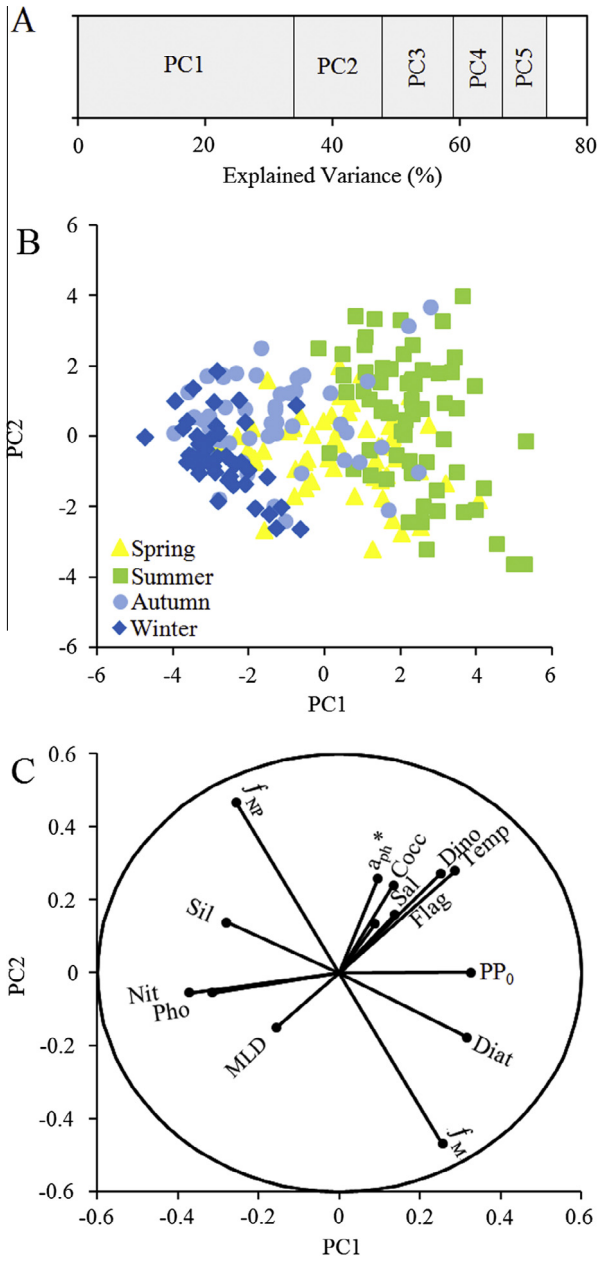

Fig. 8. Results of Principal Component Analysis showing the eigenvalues associated with the first five principal axes (A), the projection of the individual samples (categorised by season) on the plane formed by the first two principal axes (B) and the related correlation circle.

Table 2
Significant environmental and community predictors of spring and summer production as determined by multiple regression.

R^2 = 0.19 *df* = 39	Coeff.	*T*	Sign.
(A) PP_0 (Spring, n = 56)			
Intercept	−214.1		
Flagellates	79	3.55	p = 0.001
R^2 = 0.32 *df* = 39			
(B) PP_{eu} (Spring, n = 56)			
Intercept	−810.7		
Flagellates	336	−2.94	p = 0.005
Nitrate	−25.3	−2.60	p = 0.012
a^*_{ph}	7977	2.55	p = 0.014
R^2 = 0.26 *df* = 48			
(C) PP_0 (Summer, n = 65)			
Intercept	2442		
Salinity	−70	−3.11	p = 0.003
a^*_{ph}	−2913	3.41	p = 0.001
Diatoms	19.3	2.39	p = 0.020
R^2 = 0.43 *df* = 48			
(D) PP_{eu} (Summer, n = 65)			
Intercept	−8521		
a^*_{ph}	−27,403	6.65	p < 0.001
Diatoms	94	2.40	p = 0.019
Salinity	−243	−2.24	p = 0.028
R^2 = 0.22 *df* = 39			
(E) PP_M (Spring, n = 56)			
Intercept	−119.1		
Flagellates	40	2.65.65	p = 0.010
Diatoms	7.7	2.05	p = 0.046
R^2 = 0.22 *df* = 39			
(F) PP_{NP} (Spring, n = 56)			
Intercept	−67.1		
Flagellates	28.1	−3.04	p = 0.004
Nitrate	−1.27	−1.64	p = 0.047
R^2 = 0.31 *df* = 48			
(G) PP_M (Summer, n = 65)			
Intercept	1479		
Diatoms	15.1	2.74	p = 0.008
Salinity	−41	−2.81	p = 0.007
Coccolithophores	−13.8	−2.44	p = 0.017
R^2 = 0.37 *df* = 48			
(H) PP_{NP} (Summer, n = 65)			
Intercept	−14.62		
a^*_{ph}	−1172	3.59	p = 0.001
Silicate	5.6	4.04	p < 0.001
Nitrite	−43	−2.07	p = 0.042

Recent research from weekly sampling at L4 has shown fluctuation between winter when station L4 acts as a CO_2 source to the atmosphere, and spring and summer when it acts as a CO_2 sink (Kitidis et al., 2012).

Estimates of total annual production have also previously been made for the WEC. Notably, Joint and Groom (2000) applied a simple empirical algorithm to estimate primary production at E1 based on satellite-derived chlorophyll concentrations; however, their analysis was restricted to the period April to September inclusive to reduce the effects of suspended particulate material on chlorophyll retrieval during winter. Even so these authors report production estimates of 122 and 124 g C m^{-2} in 1998 and 1999, respectively, with the highest carbon fixation in spring. Based on mixing rates and the transfer of inorganic phosphate through the thermocline, Pingree and Pennycuick (1975) similarly estimated ca. 100 g C m^{-2} annually at E1. The only estimate at station L4 to date has been from 2001 where ^{14}C *in situ* measurements yielded ca. 82 g C m^{-2} (Woods, 2003). Thus our estimates (91–124 mg C m^{-2}) are more in line with past E1 estimates and suggest previous estimates for L4 have been underestimated, most likely since Woods (2003) data were based on a non-standard 24 h incubation method which, given dark loss of fixed carbon, is expected to under-estimate gross production. Importantly, our results build on such past estimates to demonstrate substantial inter-annual variability in the timing and magnitude of the spring bloom, (Figs. 2A, 4 and 5). The two years with the highest annual carbon fixation budgets (2005 and 2006) also had the highest total spring budgets (Fig. 8). Furthermore there was no significant difference in mean summer a_{ph} biomass between years (Fig. 3B) although summer blooms varied substantially in their temporal profile. As such, whilst the summer period is responsible for most of the annual carbon fixation at L4, variability in the spring bloom ultimately appears to drive the total annual productivity given the higher variability in total nutrient supply for spring blooms than for summer blooms.

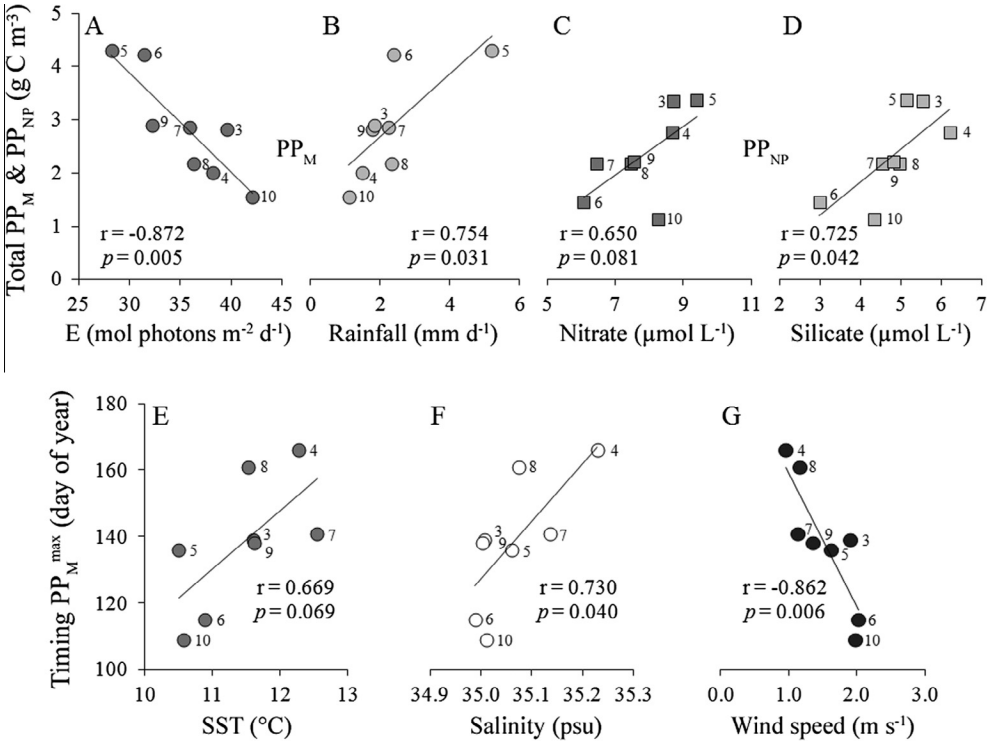

Fig. 9. Significant predictors of seasonal carbon fixation budgets and the timing of the spring maximum. Regressions between total spring PP_M (g C m^{-3}) and both mean irradiance (mol photons m^{-2} d^{-1}, A) and mean rainfall (mm d^{-1}, B) for the same period; spring PP_{NP} (g C m^{-3}) and both mean nitrate (µmol L^{-1}, C) and silicate winter concentrations (µmol L^{-1}, D); timing of the spring PP_M^{max} (day of year) and mean spring SST (°C, E), salinity (psu, F) and wind speed (m s^{-1}, G). Year numbers are indicated for each point.

Table 3
Phytoplankton taxa explaining >3% of the variability in PP_M (A) and PP_{NP} (B) at L4, as determined by a multiple regression. Approximate size range is indicated according to Tomas (1996).

Species	Group	*T*	*p*	R^2 (%)	Size range (µm)
(A) PP_M					
Rhizosolenia sp.	Diat	7.70	<0.001	28.7	4–25 (width)
Guinardia delicatula	Diat	5.87	<0.001	12.7	9–22 (diameter)
Dinophysis acuta	Dino	5.87	<0.001	6.6	43–60 (width)
Guinardia flaccida	Diat	5.07	<0.001	3.9	42–90 (diameter)
Thalassiothrix sp.	Diat	4.50	<0.001	3.8	>100 (length)
Karenia mikimotoi	Dino	4.35	<0.001	3.3	14–35 (width)
+32 taxa			<0.050	+28.4	
(B) PP_{NP}					
Karenia mikimotoi	Dino	10.26	<0.001	29.3	14–35 (width)
Rhizosolenia sp.	Diat	4.12	<0.001	6.8	4–25 (width)
Diploneis crabro	Diat	−4.03	<0.001	5.2	30–50 (width)
Prorocentrum cordatum	Dino	6.07	<0.001	4.5	8–22 (diameter)
Haslea cf warwickae	Diat	−5.77	<0.001	5.3	>100 (length)
Heterocapsa sp.	Dino	4.24	<0.001	3.4	8–12 (width)
+17 taxa			<0.050	+19.4	

4.2. Dependence of primary production on phytoplankton community composition

Both PP_M and PP_{NP} exhibited bi-modal peaks in production throughout (Fig 5), but importantly had different seasonal and inter-annual trends from 2003–2010 with smaller size group contributing 48% of the carbon fixation in surface waters and even higher relative contribution in autumn. Globally PP_{NP} has recently been shown to account for between 95% (Brewin et al., 2010a) and 68% (Uitz et al., 2010) of total annual carbon fixation. Contribution of micro-phytoplankton to total carbon fixation is considerably greater in temperate and coastal ecosystems (Uitz et al., 2010), including the North Atlantic (McQuatters-Gollop et al., 2011). However, nano- and pico-phytoplankton appear to have relatively low biomass at station L4 (Tarran and Bruun, 2015), but significantly higher photosynthetic efficiency likely yielding higher photosynthetic rates (Barnes et al., 2014). Previous studies have reported pico-phytoplankton biomass and production to be consistently low and much less variable than larger size classes (Uitz et al., 2010), only contributing high proportions of productivity in oligotrophic gyres (Maranon et al., 2001; Moreno-Ostos et al., 2011). Nano-phytoplankton on the other hand often enhance production particularly in coastal upwelling regions (Hirata et al., 2009; Tilstone et al., 1999), due to a higher efficiency of light utilisation (Tilstone et al., 1999). In the WEC, a significant decline in PP_{NP} was observed throughout the time series (Fig. 6C), primarily driven by high summer and spring anomalies from 2003–2005 and low anomalies from 2008–2010 (Fig. 7), and replaced by PP_M dominance.

Long-term community dynamics of phytoplankton functional types in the WEC are relatively well understood. For example, from 1992–2007 at L4, flagellates were the numerically dominant functional group (Widdicombe et al., 2010), yet diatoms and dinoflagellates have much higher cellular carbon concentrations (Menden-Deuer and Lessard, 2000) and thus contribute more to total carbon fixation (Figs. 4 and 5); however, our study showed that PP_M was primarily driven by diatoms whilst PP_{NP} and not linked to a particular group, but instead associated with higher light absorption efficiency. Widdicombe et al. (2010) reported a decrease in diatoms and *Phaeocystis* sp. over the 15 years from 1992 to 2007 in the WEC, and an increase in dinoflagellates and coccolithophorids. The decrease in *Phaeocystis* sp. observed by Widdicombe et al. (2010) was particularly marked from 2004 to

2007 and the cell abundance was also low in 2008 and 2009. This may be exerting a significant effect on PP_{NP}. Though Widdicombe et al. (2010) have observed a steady decline in diatoms, there was no apparent impact on PP_M, since this appeared counter balanced in the micro-phytoplankton with an increase in dinoflagellates during summer over the time series. When PP_M was high, PP_{NP} was low (Fig. 10), presumably due to competition for resources.

Numerous studies have shown that variability of a^*_{ph} is essentially driven by pigment packaging, which in turn is altered by phytoplankton community size structure and taxon-specific pigments (Bricaud et al., 2004). As noted above, L4 has seen significant long term changes in diatom and coccolithophore abundance over time (Widdicombe et al., 2010) and spring productivity over the past decade has been primarily linked to flagellate biomass (Fig 8). Consequently, the fact that changes in mean seasonal abundance of diatoms, dinoflagellates, flagellates or coccolithophores were unrelated to inter-annual changes in seasonal budgets of primary production (Fig. 9), therefore suggests that variability of productivity we observe (and hence a^*_{ph}) is generally more strongly linked to phytoplankton functional groupings than phytoplankton size classes. Point variability in primary production over the time series, however, could be explained by individual species of diatoms and dinoflagellates (Table 2). Summer *Karenia mikimotoi* blooms have been recently shown to result in the highest contribution of any species to carbon fixation over an annual cycle in the WEC (Barnes et al., 2015). *K. mikimotoi* is typically 30 μm in size and usually considered a member of the micro-phytoplankton size class (Tomas, 1996); however, the fact that it explains the greatest proportion of the variance in PP_{NP} is surprising but could reflect (i) the close association between *K. mikimotoi* and nano-phytoplankton blooms (above) rather than a direct contribution to PP_{NP}, and or (ii) possible co-occurrence of phytoflagellates sustained by the dissolved organic matter from *K. mikimotoi* blooms. Furthermore, during the summer presence of *Rhizosolenia* sp. was also strongly related to primary production to make a significant contribution to the variance in PP_M and, to a lesser extent, in PP_{NP}. However, whilst diatoms often form large chains that are typically retained in the 10 μm filters, single cells can still pass through this pore size and potentially introduce bias in PP_{NP}. Such explanations are presently impossible to fully resolve and clearly warrant further investigation; however, fundamentally, long term decline in either of these species has been found and thus cannot ultimately explain the observed patterns in PP_{NP}.

4.3. Dependence of primary production on abiotic factors

The dependence of phytoplankton photo-physiological properties on abiotic factors, such as irradiance, temperature and nutrients has been extensively documented (Geider et al., 1996; Stramski et al., 2002) but few direct observations have been made in the field (Babin et al., 1996; Bouman et al., 2003; Maranon et al., 2003; Moore et al., 2005). From the PCA, higher PP_0 and PP_M were linked to the seasonal increase in temperature (Fig. 8) whilst from the stepwise multiple regression, decreases in salinity in summer lead to higher PP_{eu}, PP_0 and PP_M. During summer low saline intrusions have previously been shown to alleviate nutrient limitation and induce an increase in phytoplankton biomass in coastal waters (Smayda, 1997) which in turn may affect the density structure, and hence the circulation of phytoplankton. However, whilst salinity was a significant predictor of L4 production during summer, it only explained a small proportion of the variance in productivity whilst temperature was not found to be a significant predictor of instantaneous production for specific seasons (Table 2).

Temperature controls the enzymatic processes associated with photosynthesis, and in water temperatures below 20 °C such as those at L4, the optimum daily photosynthetic rate increases linearly as a function of temperature (Behrenfeld and Falkowski, 1997; Eppley and Renger, 1974). Whilst the relationship between temperature and photosynthesis has been used to parameterise the physiological state variable in many satellite based in many primary production models (Behrenfeld and Falkowski, 1997; Morel, 1991), these are inaccurate at L4 (Barnes et al., 2014), possibly since the variability in PP_0 and PP_{eu} at weekly time scales is driven principally by the phytoplankton community composition rather than temperature, even though these parameters can be coupled. New parameterisation of photosynthetic parameters based on size classes (Uitz et al., 2008) and/or temperature specific relationships at L4 (e.g. Xie et al., 2015) may therefore improve these relationships, but require further testing in coastal waters.

Spring productivity was highly variable over the time series yet several significant relationships were found between abiotic factors and total spring production. PP_{NP} was significantly positively related to mean winter silicate and, apart from in 2010, was strongly related to winter nitrate (Fig. 9). Furthermore both winter nitrate and silicate were higher during 2003–2005 than from 2006–2010 and thus potentially explain the temporal decline in PP_{NP} from 2003–2010. Whilst high nutrients are generally thought to promote larger cells such as diatoms (McAndrew et al., 2007; Poulton et al., 2006), recent studies have observed a stimulating effect of nitrate on the growth rates of smaller cells (Huete-Ortega et al., 2011). In the presence of decreasing winter nitrate, micro-phytoplankton may dominate the uptake of nitrate compared to nano- + pico-phytoplankton, which would also cause a decline in PP_{NP} (Fig. 10). Changes in nutrient concentrations in the WEC in the past decade have therefore had a significant effect on PP_{NP} and carbon fixation as a whole (Fig. 8, Table 2).

Climate change induced warmer SST are expected to result in changes in stratification in the North Atlantic and could result in earlier spring blooms of higher magnitude (Behrenfeld et al., 2006; Sarmiento et al., 2004). These blooms may then extend throughout the summer (Raitsos et al., 2014) especially in areas with thermal fronts and bathymetric ridges (Tilstone et al., 2014) which act as a nutrient supply to the photic zone. In our study, increased SST and decreased wind speeds were associated with later blooms and mixed layer depth was unrelated to either the timing of the blooms or the annual carbon fixation. Later timing of the spring bloom coupled with increases in precipitation forced by changes in the jet stream (Francis and Vavrus, 2012; Rahmstorf and Coumou, 2011) would lead to spring blooms that continue into the summer in these coastal waters; a situation which occurred in both 2011 (Queirós et al., 2015) and 2012 (Zhang et al., 2015) at station L4. During years with high summer precipitation, there was an increase in both micro- and total primary production (e.g. 2004, 2008, 2009; Figs. 4, 5, and 9B). Longer bloom duration would enhance the drawdown of CO_2 in coastal regions of the WEC. However, this is highly dependent on the dominant phytoplankton group; for example increased precipitation can trigger the potential HAB *Karenia mikimotoi* (Barnes et al., 2015), and in this case the fixed carbon maybe released back to the atmosphere or accumulate in the sediment causing potential anoxic effects. Even so, our observations for L4 contrast with other regions (such as the North Sea, e.g. Wiltshire et al. (2008), suggesting that long term effects of increases in temperature may be somewhat localised.

Changes in production may ultimately be more related to altered community structure (Richardson and Schoeman, 2004) than abiotic factors (see also above for point measurements). Meteorological variables such as rainfall and irradiance were also observed to affect the total spring production budget between years (Fig. 9). Higher mean spring irradiance was however, associated with lower absolute PP_M. This relationship seems counter-intuitive, but it could be possible that the turbulent conditions associated with high winds and clear skies, i.e. high

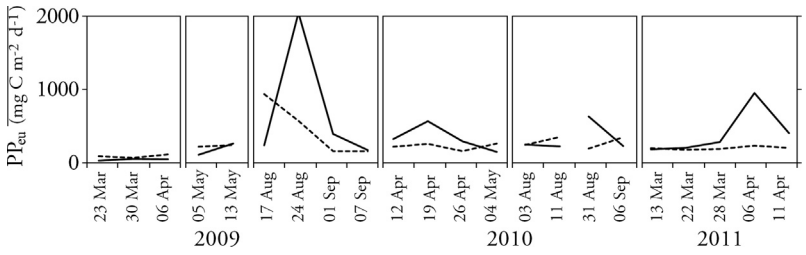

Fig. 10. Size fractionated primary production data collected from the Western English Channel during 2009–2011 for micro- (solid line) and nano + pico-phytoplankton (dashed line).

irradiance, inhibit the onset of PP_M. Higher PP_M was associated with high rainfall and therefore cloud cover and lower irradiance, which is associated with lower wind speeds and promote the transition from winter mixing to spring stratification of the water column to trigger PP_M. In this case knowledge of physiology that is not accounted for by a^*_{ph} (i.e. the quantum yield), and how it varies amongst taxa and in response to short-term environmental fluctuations (e.g. Moore et al., 2006) is likely critical to reconcile our observations. Additionally, it is possible that during years with high irradiance, blooms develop much quicker and have a much shorter duration (Cushing, 1989), which could be missed by the weekly sampling periodicity. To further enhance the frequency of sampling, optical based algorithms of primary production such as that of Barnes et al. (2014), could be used in conjunction with autonomous measurements of absorption from WetLabs ac9 or acS type instruments deployed on mooring or in continuous data acquisition mode on ships.

5. Conclusions

We have demonstrated how phytoplankton absorption can provide an important means of estimating coastal primary production, and can be successfully applied to measurements of $a_{ph}(\lambda)$ to derive long-term time series of both surface and depth-integrated primary production. Combined with knowledge of size-fractionated phytoplankton absorption, this method can also be used to derive production time series for different size classes, which can then be used to investigate the drivers of long-term trends in primary production. Over the past decade at station L4, PP_{eu} varied between 91–128 g C m^{-2} d^{-1} whilst PP_0 varied between 9.9–18 g C m^{-3} d^{-1}. Nano- and pico-phytoplankton contributed equally to the annual primary production as micro-phytoplankton. The weekly variability in primary production was related to phytoplankton species community composition. Species such as *Karenia mikimotoi* and *Rhizosolenia* sp. (micro-phytoplankton size class) explained much of this variability. Significant repeat cycles in PP_{NP} and PP_M were evident at 6 and 4 months, illustrating bi-modal peaks in the production of both micro- and nano + pico-phytoplankton, which were stronger in some years (e.g. 2007, 2008) than others years (e.g. 2004, 2005, 2006 & 2010). PP_{NP} and PP_M were decoupled, and only when PP_{NP} was low did PP_M become higher (Fig. 10). A decline in PP_{NP} over the 8-year time series was observed, which was related to a decrease in winter nitrate and silicate and *Phaeocystis* sp. from 2003–2010. On a seasonal basis, PP_M remained stable from 2003 to 2010, and was enhanced in summer during periods of high rainfall and river run-off. An increase in SST and salinity, and decrease in wind speeds were associated with later maxima in PP_M. The decadal variability in primary productivity at L4 would suggest that future increases in temperature and decrease in wind speeds, would induce the spring peak in production to occur later. This in conjunction with increased summer precipitation forced by changes in the jet stream, could continue throughout the summer at this coastal site.

Acknowledgements

We thank the crew of RV Plymouth Quest. MKB was supported by a NERC studentship (NE/F012608/1). GHT and VMV were supported by the European Union contract Information System on the Eutrophication of our Coastal Seas (ISECA) (Contract No. 07-027-FR-ISECA) funded by INTERREG IVA 2 Mers Seas Zeeen Cross-border Cooperation Programme 2007–2013. TJSM and CW were supported by the NERC National Capability Western English Channel Observatory. JB was supported by the FP7 project Green Seas (Contract No. 265294).

References

Araujo, J.N., Mackinson, S., Stanford, R.J., Sims, D.W., Southward, A.J., Hawkins, S.J., Ellis, J.R., Hart, P.J.B., 2006. Modelling food web interactions, variation in plankton production, and fisheries in the western English Channel ecosystem. Marine Ecology Progress Series 309, 175–187.

Babin, M., Morel, A., Claustre, H., Bricaud, A., Kolber, Z., Falkowski, P.G., 1996. Nitrogen- and irradiance-dependent variations of the maximum quantum yield of carbon fixation in eutrophic, mesotrophic and oligotrophic marine systems. Deep-Sea Research Part I: Oceanographic Research Papers 43, 1241–1272.

Barnes, M.K., Tilstone, G.H., Smyth, T.J., Suggett, D.J., Astoreca, R., Lancelot, C., Kromkamp, J.C., 2014. Absorption-based algorithm of primary production for total and size-fractionated phytoplankton in coastal waters. Marine Ecology Progress Series 504, 1–12.

Barnes, M.K., Tilstone, G.H., Smyth, T.J., Widdicombe, C.E., Gloel, J., Robinson, C., Kaiser, J., Suggett, D.J., 2015. Drivers and effects of *Karenia mikimotoi* blooms in the western English Channel. Progress in Oceanography 137, 456–469.

Bauer, J.E., Cai, W.-J., Raymond, P.A., Bianchi, T.S., Hopkinson, C.S., Regnier, P.A.G., 2013. The changing carbon cycle of the coastal ocean. Nature 504, 61–70.

Behrenfeld, M.J., Falkowski, P.G., 1997. Photosynthetic rates derived from satellite-based chlorophyll concentration. Limnology and Oceanography 42, 1–20.

Behrenfeld, M.J., O'Malley, R.T., Siegel, D.A., McClain, C.R., Sarmiento, J.L., Feldman, G.C., Milligan, A.J., Falkowski, P.G., Letelier, R.M., Boss, E.S., 2006. Climate-driven trends in contemporary ocean productivity. Nature 444, 752–755.

Boalch, G.T., 1987. Changes in the phytoplankton of the western English Channel in recent years. British Phycological Journal 22, 225–235.

Boalch, G.T., Harbour, D.S., Butler, E.I., 1978. Seasonal phytoplankton production in the western English Channel 1964–1974. Journal of the Marine Biological Association of the United Kingdom 58, 943–953.

Bouman, H.A., Platt, T., Sathyendranath, S., Li, W.K.W., Stuart, V., Fuentes-Yaco, C., Maass, H., Horne, E.P.W., Ulloa, O., Lutz, V., Kyewalyanga, M., 2003. Temperature as indicator of optical properties and community structure of marine phytoplankton: implications for remote sensing. Marine Ecology Progress Series 258, 19–30.

Bouman, H., Platt, T., Sathyendranath, S., Stuart, V., 2005. Dependence of light-saturated photosynthesis on temperature and community structure. Deep-Sea Research Part I-Oceanographic Research Papers 52, 1284–1299.

Brewin, R.J.W., Lavender, S.J., Hardman-Mountford, N.J., 2010a. Mapping size-specific phytoplankton primary production on a global scale. Journal of Maps, 448–462.

Brewin, R.J.W., Sathyendranath, S., Hirata, T., Lavender, S.J., Barciela, R.M., Hardman-Mountford, N.J., 2010b. A three-component model of phytoplankton size class for the Atlantic Ocean. Ecological Modelling 221, 1472–1483.

Bricaud, A., Claustre, H., Ras, J., Oubelkheir, K., 2004. Natural variability of phytoplanktonic absorption in oceanic waters: influence of the size structure of algal populations. Journal of Geophysical Research: Oceans 109, C11010, doi:11010.11029/12004JC002419.

Bruun, J., Somerfield, P., Allen, I.J., 2012. Applications of Box Jenkins Transfer Function methods to identify seasonal and longer term trends in Marine time series. ICES Journal of Marine Science 22, 1–12.
Cote, B., Platt, T., 1984. Utility of the light-saturation curve as an operational model for quantifying the effects of environmental conditions on phytoplankton photosynthesis. Marine Ecology Progress Series 18, 57–66.
Cushing, D.H., 1989. A difference in structure between ecosystems in strongly stratified waters and in those that are only weakly stratified. Journal of Plankton Research 11, 1–13.
Eloire, D., Somerfield, P.J., Conway, D.V.P., Halsband-Lenk, C., Harris, R., Bonnet, D., 2010. Temporal variability and community composition of zooplankton at station L4 in the Western Channel: 20 years of sampling. Journal of Plankton Research 32, 657–679.
Eppley, R.W., 1972. Temperature and phytoplankton growth in the sea. Fisheries Bulletin 70, 1063–1085.
Eppley, R.W., Renger, E.H., 1974. Nitrogen assimilation of an oceanic diatom in nitrogen limited continuous culture. Journal of Phycology 10, 15–23.
Francis, J.A., Vavrus, S.J., 2012. Evidence linking Arctic amplification to extreme weather in mid-latitudes. Geophysical Research Letters 39, L06801.
Garcia, V.M.T., Purdie, D.A., 1994. Primary production studies during a *Gyrodinium* cf *aureolum* (Dinophyceae) bloom in the western English Channel. Marine Biology 119, 297–305.
Geider, R.J., MacIntyre, H.L., Kana, T.M., 1996. A dynamic model of photoadaptation in phytoplankton. Limnology and Oceanography 41, 1–15.
Genner, M.J., Halliday, N.C., Simpson, S.D., Southward, A.J., Hawkins, S.J., Sims, D.W., 2010. Temperature-driven phenological changes within a marine larval fish assemblage. Journal of Plankton Research 32, 699–708.
Gregg, W.W., Carder, K.L., 1990. A simple spectral solar irradiance model for cloudless maritime atmospheres. Limnology and Oceanography 35, 1657–1675.
Groom, S., Martinez-Vicente, V., Fishwick, J., Tilstone, G., Moore, G., Smyth, T., Harbour, D., 2009. The Western English Channel observatory: optical characteristics of station L4. Journal of Marine Systems 77, 278–295.
Harding, L.W., Meeson, B.W., Fisher, T.R., 1986. Phytoplankton production in 2 east-coast estuaries – photosynthesis light functions and patterns of carbon assimilation in Chesapeake and Delaware bays. Estuarine, Coastal and Shelf Science 23, 773–806.
Henson, S.A., Sarmiento, J.L., Dunne, J.P., Bopp, L., Lima, I., Doney, S.C., John, J., Beaulieu, C., 2010. Detection of anthropogenic climate change in satellite records of ocean chlorophyll and productivity. Biogeosciences 7, 621–640.
Hirata, T., Hardman-Mountford, N.J., Barlow, R., Lamont, T., Brewin, R., Smyth, T., Aiken, J., 2009. An inherent optical property approach to the estimation of size-specific photosynthetic rates in eastern boundary upwelling zones from satellite ocean colour: an initial assessment. Progress in Oceanography 83, 393–397.
Holligan, P.M., Harris, R.P., Newell, R.C., Harbour, D.S., Head, R.N., Linley, E.A.S., Lucas, M.I., Tranter, P.R.G., Weekley, C.M., 1984. Vertical-distribution and partitioning of organic-carbon in mixed, frontal and stratified waters of the English-Channel. Marine Ecology Progress Series 14, 111–127.
Huete-Ortega, M., Calvo-Diaz, A., Grana, R., Mourino-Carballido, B., Maranon, E., 2011. Effect of environmental forcing on the biomass, production and growth rate of size-fractionated phytoplankton in the central Atlantic Ocean. Journal of Marine Systems 88, 203–213.
Joint, I., Groom, S.B., 2000. Estimation of phytoplankton production from space: current status and future potential of satellite remote sensing. Journal of Experimental Marine Biology and Ecology 250, 233–255.
Kameda, T., Ishizaka, J., 2005. Size-fractionated primary production estimated by a two-phytoplankton community model applicable to ocean color remote sensing. Journal of Oceanography 61, 663–672.
Kitidis, V., Hardman-Mountford, N.J., Litt, E., Brown, I., Cummings, D., Hartman, S., Hydes, D., Fishwick, J.R., Harris, C., Martinez-Vicente, V., Woodward, E.M.S., Smyth, T.J., 2012. Seasonal dynamics of the carbonate system in the Western English Channel. Continental Shelf Research 42, 30–40.
Kyewalyanga, M.N., Platt, T., Sathyendranath, S., Lutz, V.A., Stuart, V., 1998. Seasonal variations in physiological parameters of phytoplankton across the north Atlantic. Journal of Plankton Research 20, 17–42.
Le Quere, C., Aumont, O., Monfray, P., Orr, J., 2003. Propagation of climatic events on ocean stratification, marine biology, and CO_2: case studies over the 1979–1999 period. Journal of Geophysical Research: Oceans 108.
Levitus, S., 1982. Climatological atlas of the World Ocean. In: NOAA Professional Paper.
Lewis, M.R., Horne, E.P.W., Cullen, J.J., Oakey, N.S., Platt, T., 1984. Turbulent motions may control phytoplankton photosynthesis in the upper ocean. Nature 311, 49–50.
Llewellyn, C.A., Fishwick, J.R., Blackford, J.C., 2005. Phytoplankton community assemblage in the English Channel: a comparison using chlorophyll a derived from HPLC-CHEMTAX and carbon derived from microscopy cell counts. Journal of Plankton Research 27, 103–119.
Maranon, E., Holligan, P.M., Barciela, R., Gonzalez, N., Mourino, B., Pazo, M.J., Varela, M., 2001. Patterns of phytoplankton size structure and productivity in contrasting open-ocean environments. Marine Ecology Progress Series 216, 43–56.
Maranon, E., Behrenfeld, M.J., Gonzalez, N., Mourino, B., Zubkov, M.V., 2003. High variability of primary production in oligotrophic waters of the Atlantic Ocean: uncoupling from phytoplankton biomass and size structure. Marine Ecology Progress Series 257, 1–11.
Maranon, E., 2009. Inter-specific scaling of phytoplankton production and cell size in the field. Journal of Plankton Research 31, 929–939.
Martinez-Vicente, V., Land, P.E., Tilstone, G.H., Widdicombe, C., Fishwick, J.R., 2010. Particulate scattering and backscattering related to water constituents and seasonal changes in the Western English Channel. Journal of Plankton Research 32, 603–619.
McAndrew, P.M., Bjorkman, K.M., Church, M.J., Morris, P.J., Jachowski, N., Williams, P.J.L.B., Karl, D.M., 2007. Metabolic response of oligotrophic plankton communities to deep water nutrient enrichment. Marine Ecology Progress Series 332, 63–75.
McQuatters-Gollop, A., Reid, P.C., Edwards, M., Burkill, P.H., Castellani, C., Batten, S., Gieskes, W., Beare, D., Bidigare, R.R., Head, E., Johnson, R., Kahru, M., Koslow, J.A., Pena, A., 2011. Is there a decline in marine phytoplankton? Nature 472, E6–E7.
Menden-Deuer, S., Lessard, E.J., 2000. Carbon to volume relationships for dinoflagellates, diatoms, and other protist plankton. Limnology and Oceanography 45, 569–579.
Moore, C.M., Lucas, M.I., Sanders, R., Davidson, R., 2005. Basin-scale variability of phytoplankton bio-optical characteristics in relation to bloom state and community structure in the Northeast Atlantic. Deep-Sea Research Part I: Oceanographic Research Papers 52, 401–419.
Moore, C.M., Suggett, D.J., Hickman, A.E., Kim, Y.-N., Sharples, J., Geider, R.J., Holligan, P.M., 2006. Phytoplankton photo-acclimation and photo-adaptation in response to environmental gradients in a shelf sea. Limnology and Oceanography 51, 936–949.
Morel, A., 1991. Light and marine photosynthesis – a spectral model with geochemical and climatological implications. Progress in Oceanography 26, 263–306.
Moreno-Ostos, E., Fernandez, A., Huete-Ortega, M., Mourino-Carballido, B., Calvo-Diaz, A., Moran, X.A.G., Maranon, E., 2011. Size-fractionated phytoplankton biomass and production in the tropical Atlantic. Scientia Marina 75, 379–389.
Peter, K.H., Sommer, U., 2012. Phytoplankton cell size: intra- and interspecific effects of warming and grazing. PLosOne 7, e49632.
Pingree, R., 1980. Physical oceanography of the Celtic Sea and English Channel. The North–West European Shelf Seas: The Sea Bed and the Sea in Motion. II. Physical and Chemical Oceanography and Physical Resources, 415–465.
Pingree, R.D., Pennycuick, L., 1975. Transfer of heat, fresh water and nutrients through the seasonal thermocline. Journal of Marine Biological Association of UK 55, 261–274.
Platt, T., Sathyendranath, S., 1993. Estimators of primary production for interpretation of remotely-sensed data on ocean color. Journal of Geophysical Research: Oceans 98, 14561–14576.
Poulton, A.J., Holligan, P.M., Hickman, A., Kim, Y.N., Adey, T.R., Stinchcombe, M.C., Holeton, C., Root, S., Woodward, E.M.S., 2006. Phytoplankton carbon fixation, chlorophyll-biomass and diagnostic pigments in the Atlantic Ocean. Deep-Sea Research Part II: Topical Studies in Oceanography 53, 1593–1610.
Queirós, A.M., Stephens, N., Cook, R., Ravaglioli, C., Nunes, J., Dashfield, S., Harris, C., Tilstone, G.H., Fishwick, J., Somerfield, P., Widdicombe, S., 2015. Can benthic community structure be used to predict bioturbation in ecosystems? Progress in Oceanography 137, 559–569.
Rahmstorf, S., Coumou, D., 2011. Increase of extreme events in a warming world. Proceedings of the National Academy of Sciences 108, 17905–17909.
Raitsos, D.E., Pradhan, Y., Lavender, S., Hoteit, I., McQuatters-Gollop, A., Reid, P.C., Richardson, A.J., 2014. From silk to satellite: half a century of ocean colour anomalies in the Northeast Atlantic. PLoS One 12457, 1–14.
Reed, R., 1977. On estimating insolation over the ocean. Journal of Physical Oceanography 7, 482–485.
Rees, A.P., Hope, S.B., Widdicombe, C.E., Dixon, J.L., Woodward, E.M.S., Fitzsimons, M.F., 2009. Alkaline phosphatase activity in the western English Channel: elevations induced by high summertime rainfall. Estuarine, Coastal and Shelf Science 81, 569–574.
Richardson, A.J., Schoeman, D.S., 2004. Climate impact on plankton ecosystems in the Northeast Atlantic. Science 305, 1609–1612.
Sarmiento, J.L., Slater, R., Barber, R., Bopp, L., Doney, S.C., Hirst, A.C., Kleypas, J., Matear, R., Mikolajewicz, U., Monfray, P., Soldatov, V., Spall, S.A., Stouffer, R., 2004. Response of ocean ecosystems to climate warming. Global Biogeochemical Cycles 18.
Sathyendranath, S., Platt, T., Caverhill, C.M., Warnock, R.E., Lewis, M.R., 1989. Remote-sensing of oceanic primary production – computations using a spectral model. Deep-Sea Research Part A: Oceanographic Research Papers 36, 431–453.
Sharples, J., Moore, C.M., Rippeth, T.P., Holligan, P.M., Hydes, D.J., Fisher, N.R., Simpson, J.H., 2001. Phytoplankton distribution and survival in the thermocline. Limnology and Oceanography 46, 489–496.
Shumway, R.H., Stoffer, D.S., 2010. Time Series Analysis and Its Applications: With R Examples. Springer, New York.
Sieburth, J.M., Smetacek, V., Lenz, J., 1978. Pelagic ecosystem structure – heterotrophic compartments of plankton and their relationship to plankton size fractions – comment. Limnology and Oceanography 23, 1256–1263.
Smayda, T.J., 1997. Harmful algal blooms: their ecophysiology and general relevance to phytoplankton blooms in the sea. Limnology and Oceanography 42, 1137–1153.
Smyth, T.J., Fishwick, J.R., Al-Moosawi, L., Cummings, D.G., Harris, C., Kitidis, V., Rees, A., Martinez-Vicente, V., Woodward, E.M.S., 2010. A broad spatio-temporal view of the Western English Channel observatory. Journal of Plankton Research 32, 585–601.
Southward, A.J., Langmead, O., Hardman-Mountford, N.J., Aiken, J., Boalch, G.T., Dando, P.R., Genner, M.J., Joint, I., Kendall, M.A., Halliday, N.C., Harris, R.P.,

Leaper, R., Mieszkowska, N., Pingree, R.D., Richardson, A.J., Sims, D.W., Smith, T., Walne, A.W., Hawkins, S.J., 2005. Long-term oceanographic and ecological research in the western English Channel. In: Southward, A.J., Tyler, P.A., Young, C.M., Fuiman, L.A. (Eds.), Advances in Marine Biology, vol. 47, pp. 1–105.

Stramski, D., Sciandra, A., Claustre, H., 2002. Effects of temperature, nitrogen, and light limitation on the optical properties of the marine diatom *Thalassiosira pseudonana*. Limnology and Oceanography 47, 392–403.

Tarran, T.A., Bruun, J.T., 2015. Nanoplankton and picoplankton in the Western English Channel: abundance and seasonality from 2007–2013. Progress in Oceanography 137, 446–455.

Tassan, S., Ferrari, G.M., 1995. An alternative approach to absorption measurements of aquatic particles retained on filters. Limnology and Oceanography 40, 1358–1368.

Tassan, S., Ferrari, G.M., 1998. Measurement of light absorption by aquatic particles retained on filters: determination of the optical pathlength amplification by the 'transmittance-reflectance' method. Journal of Plankton Research 20, 1699–1709.

Tett, P., Gilpin, L., Svendsen, H., Erlandsson, C.P., Larsson, U., Kratzer, S., Fouilland, E., Janzen, C., Lee, J.Y., Grenz, C., Newton, A., Ferreira, J.G., Fernandes, T., Scory, S., 2003. Eutrophication and some European waters of restricted exchange. Continental Shelf Research 23, 1635–1671.

Tilstone, G.H., Figueiras, F.G., Fermin, E.G., Arbones, B., 1999. Significance of nanophytoplankton photosynthesis and primary production in a coastal upwelling system (Ria de Vigo, NW Spain). Marine Ecology Progress Series 183, 13–27.

Tilstone, G.H., Figueiras, F.G., Lorenzo, L.M., Arbones, B., 2003. Phytoplankton composition, photosynthesis and primary production during different hydrographic conditions at the Northwest Iberian upwelling system. Marine Ecology Progress Series 254, 89–104.

Tilstone, G.H., Smyth, T.J., Gowen, R.J., Martinez-Vicente, V., Groom, S.B., 2005. Inherent optical properties of the Irish Sea and their effect on satellite primary production algorithms. Journal of Plankton Research 27, 1127–1148.

Tilstone, G.H., Miller, P.I., Brewin, R.J.W., Priede, I.G., 2014. Enhancement of primary production in the North Atlantic outside of the spring bloom, identified by remote sensing of ocean colour and temperature. Remote Sensing of Environment 146, 77–86.

Tomas, C.R., 1996. Identifying Marine Diatoms and Dinoflagellates. Academic Press, New York.

Uitz, J., Huot, Y., Bruyant, F., Babin, M., Claustre, H., 2008. Relating phytoplankton photophysiological properties to community structure on large scales. Limnology and Oceanography 53, 614–630.

Uitz, J., Claustre, H., Gentili, B., Stramski, D., 2010. Phytoplankton class-specific primary production in the world's oceans: seasonal and interannual variability from satellite observations. Global Biogeochemical Cycles 24.

Uncles, R., Stephens, J., 1990. The structure of vertical current profiles in a macrotidal, partly-mixed estuary. Estuaries 13, 349–361.

Widdicombe, C.E., Archer, S.D., Burkill, P.H., Widdicombe, S., 2002. Diversity and structure of the microplankton community during a coccolithophore bloom in the stratified northern North Sea. Deep-Sea Research Part II: Topical Studies in Oceanography 49, 2887–2903.

Widdicombe, C.E., Eloire, D., Harbour, D., Harris, R.P., Somerfield, P.J., 2010. Long-term phytoplankton community dynamics in the Western English Channel. Journal of Plankton Research 32, 643–655.

Wiltshire, K.H., Malzahn, A.M., Wirtz, K., Greve, W., Janisch, S., Mangelsdorf, P., Manly, B.F.J., Boersma, M., 2008. Resilience of North Sea phytoplankton spring bloom dynamics: an analysis of long-term data at Helgoland Roads. Limnology and Oceanography 53, 1294–1302.

Woods, K., 2003. Development and assessment of novel techniques to measure primary production in the Celtic Sea and English Channel. In: School of Earth and Ocean Science. University of Southampton, UK.

Xie, Y., Tilstone, G.H., Widdicombe, C., Woodward, E.M.S., Harris, C., Barnes, M.K., 2015. Effects of increases in temperature and nutrients on phytoplankton community structure and photosynthesis in the Western English Channel. Marine Ecology Progress Series 519, 61–73.

Zhang, Q., Warwick, R.M., McNeill, C.L., Widdicombe, C.E., Sheehan, A., Widdicombe, S., 2015. An unusually large phytoplankton spring bloom drives rapid changes in benthic diversity and ecosystem function. Progress in Oceanography 137, 533–545.